Generalized-Extended-State-Observer and Equivalent-Input-Disturbance Methods for Active Disturbance Rejection: Deep Observation and Comparison

Jinhua She, *Fellow, IEEE*, Kou Miyamoto, *Member, IEEE*, Qing-Long Han, *Fellow, IEEE*, Min Wu, *Fellow, IEEE*, Hiroshi Hashimoto, *Member, IEEE*, and Qing-Guo Wang

***Abstract*—Active disturbance-rejection methods are effective in estimating and rejecting disturbances in both transient and steady-state responses. This paper presents a deep observation on and a comparison between two of those methods: the generalized extended-state observer (GESO) and the equivalent input disturbance (EID) from assumptions, system configurations, stability conditions, system design, disturbance-rejection performance, and extensibility. A time-domain index is introduced to assess the disturbance-rejection performance. A detailed observation of disturbance-suppression mechanisms reveals the superiority of the EID approach over the GESO method. A comparison between these two methods shows that assumptions on disturbances are more practical and the adjustment of disturbance-rejection performance is easier for the EID approach than for the GESO method.**

***Index Terms*—Active disturbance-rejection control (ADRC), disturbance observer (DOB), equivalent input disturbance (EID), extended-state observer (ESO), generalized extended-state observer (GESO).**

Manuscript received April 17, 2022; revised June 7, 2022; accepted June 21, 2022. This work was supported in part by the JSPS (Japan Society for the Promotion of Science) KAKENHI (20H04566, 22H03998), the National Natural Science Foundation of China (61873348), the Natural Science Foundation of Hubei Province, China (2020CFA031), and Wuhan Applied Foundational Frontier Project (2020010601012175). Recommended by Associate Editor Tao Yang. *(Corresponding author: Jinhua She.)*

Citation: J. She, K. Miyamoto, Q.-L. Han, M. Wu, H. Hashimoto, and Q.-G. Wang, "Generalized-extended-state-observer and equivalent-input-disturbance methods for active disturbance rejection: Deep observation and comparison," *IEEE/CAA J. Autom. Sinica*, vol. 10, no. 4, pp. 957–968, Apr. 2023.

J. She is with the School of Engineering, Tokyo University of Technology, Hachioji, Tokyo 192-0982, Japan (e-mail: she@stf.teu.ac.jp).

K. Miyamoto is with the Institute of Technology, Shimizu Corporation, Koto, Tokyo 135-0044, Japan (e-mail: kou_miyamoto@shimz.co.jp).

Q.-L. Han is with the School of Science, Computing and Engineering Technologies, Swinburne University of Technology, Melbourne, VIC 3122, Australia (e-mail: qhan@swin.edu.au).

M. Wu is with the School of Automation, China University of Geosciences, Wuhan 430074, the Hubei Key Laboratory of Advanced Control and Intelligent Automation for Complex Systems, and the Engineering Research Center of Intelligent Technology for Geo-Exploration, Ministry of Education, Wuhan 430074, China (e-mail: wumin@cug.edu.cn).

H. Hashimoto is with the School of Industrial Technology, Advanced Institute of Industrial Technology, Tokyo 140-0011, Japan (e-mail: hashimoto @aiit.ac.jp).

Q.-G. Wang is with Institute of Artificial Intelligence and Future Networks, Beijing Normal University, Zhuhai 519087; Guangdong Key Lab of AI and Multi-Modal Data Processing, Guangdong Provincial Key Laboratory of Interdisciplinary Research and Application for Data Science; and BNU-HKBU United International College, Zhuhai 519087, China (e-mail: wang qingguo@bnu.edu.cn).

Color versions of one or more of the figures in this paper are available online at http://ieeexplore.ieee.org.

Digital Object Identifier 10.1109/JAS.2022.105929

I. Introduction

IMPROVING accuracy, reducing costs, and fastering response speed are essential in advanced motion control [1]. Disturbances, nonlinearities, and uncertainties in a mechatronic system hinder addressing those challenges. Note that, under a suitable control system setting, a disturbance-rejection method takes nonlinearities and uncertainties as a disturbance, and estimates and compensates for them. The performance of disturbance rejection is an important figure of merit for a motion-control system.

A significant number of studies have been devoted to exploring possible methodologies of disturbance rejection. The approaches can be divided into two categories: one suppresses the sensitivity function of a system that results in a prescribed disturbance-attenuation level, and the other actively estimates and compensates for a disturbance. Since the latter has a potential for satisfactory disturbance rejection in both transient and steady-state responses, it has thrown new light on the subject.

Active disturbance-rejection control (ADRC) [2]–[4] is a widely used method that directly estimates and compensates for a disturbance. The extended-state-observer (ESO) method was devised for the ADRC to produce a compensation term in a simple, effective way [2]. The generalized ESO (GESO) method was proposed to extend the ADRC to handle a wide class of plants [5], [6]. These methods have been extensively analyzed (for example, [7]–[9]) and widely applied in control engineering (for example, [10]–[12]).

The disturbance observer (DOB) [13], [14] is another common method to actively reject disturbances. The DOB method directly creates a disturbance estimate on a control input channel to ease disturbance compensation. However, it requires an inverse model of a plant. This narrows the range of its applications. The equivalent-input-disturbance (EID) approach was then devised to eliminate this constraint [15]. It integrates a control input and the information about a state observer of a plant to produce an estimate of a disturbance.

The methods of actively estimating and rejecting disturbances use estimation techniques. Some articles focused on this point and presented a systematic view of these methods (for example, [1] and [16]).

While both the GESO and EID methods are active disturbance-rejection methods, there are differences in philosophies, applicable conditions, and control-system design. This study carried out a deep observation of the GESO and EID methods to elucidate why the methods can reject disturbances and what differences are between them.

In this paper, for a signal $v(t) \in \mathbb{R}^m$, $\|v(t)\|_2 = \sqrt{v^T(t)v(t)}$, $\|v\|_\infty = \sup_{t\geq 0}\{|v_1(t)|, |v_2(t)|, \ldots, |v_m(t)|\}$, and $V(s)$ is the Laplace transform of $v(t)$. For a system $G(s)$, $\|G\|_\infty = \sup_{0\leq\omega\leq\infty} \sigma_{\max}[G(j\omega)]$ and $\sigma_{\max}(G)$ is the maximum singular value of G. The H_∞ norm of a system indicates the worst-case effect of the input on the output.

II. Performance Assessment for Disturbance-Rejection Methods

The technology of control-performance assessment is important to evaluate the effectiveness of a control system. The Bode plots of a transfer function from a disturbance to a disturbance-estimation error [6] or a transfer function from a disturbance to an output [17], the ratio of a transfer function from an input to an output and that from a disturbance to the output [18], the phase margin and the crossover frequency of a closed-loop system [19], and other measures were proposed to evaluate active-disturbance-rejection performance in the frequency domain [20], [21].

On the other hand, a linear-quadratic Gaussian benchmark is a time-domain index [22] that is widely used for disturbance rejection

$$J_{\text{LQG}} = \int_{T_s}^{T_f} \left\{ y^T(t)y(t) + \gamma_{\text{LQG}} u^T(t)u(t) \right\} dt \tag{1}$$

where $y(t)$ is an output caused by a disturbance; $u(t)$ is a control input; γ_{LQG} (>0) is a constant; and T_s and T_f are the start and finish times of the evaluation, respectively.

Compared to reference tracking, disturbance rejection has its own peculiarities. Incorporating a disturbance estimate may cause large peaks in a control input and the state of a system during a transient response, which is called a peaking phenomenon [23]. This phenomenon degrades control performance and should be mitigated appropriately. Thus, the evaluation of a peaking phenomenon is also important for active disturbance rejection and a time-domain index

$$J_{\text{peak}} = \|y\|_\infty^2 + \gamma_{\text{peak}}\|u\|_\infty^2 \tag{2}$$

can be used for this purpose, where γ_{peak} (>0) is a constant.

This study combined (1) and (2) to construct the following index:

$$J = J_{\text{LQG}} + \lambda J_{\text{peak}} \tag{3}$$

and used it to assess disturbance-rejection performance. λ (>0) in (3) is a constant.

III. An Illustrative Example

First, a numerical example illustrates these methods to provide an intuitive understanding of them.

Consider a plant

$$\begin{cases} \dot{x}_1(t) = x_2(t) + d(t) \\ \dot{x}_2(t) = -x_1(t) - x_2(t) + u(t) \\ y(t) = x_1(t) \end{cases} \tag{4}$$

where $x(t) = [x_1(t), x_2(t)]^T$ is the state, $u(t)$ is the control input, $y(t)$ is the output, and $d(t)$ is an exogenous disturbance.

A. Active Disturbance-Rejection Control Methods

The ESO and GESO are the two main methods used in ADRC. As explained in [3], the ESO method takes

$$x_{a1}(t) = y(t) \tag{5}$$

and considers Plant (4) to be

$$\begin{cases} \dot{x}_{a1}(t) = x_{a2}(t) \\ \dot{x}_{a2}(t) = u(t) + d_a(t) \\ \dot{x}_{a3}(t) = \dot{d}_a(t) \\ y(t) = x_{a1}(t) \end{cases} \tag{6}$$

where

$$d_a(t) = -x_{a1}(t) - x_{a2}(t) + [d(t) + \dot{d}(t)] \tag{7}$$

is a lumped disturbance on the control-input channel that has the same effect on the output as the combination of $d(t)$, $x_{a1}(t)$, and $x_{a2}(t)$ do. $x_{a3}(t)$ is an extended state that describes the lumped disturbance. Since $\dot{d}_a(t)$ is unknown, it is simply ignored [2], [24] by letting

$$\dot{d}_a(t) = 0. \tag{8}$$

An ESO

$$\begin{cases} \dot{\hat{x}}_{a1}(t) = \hat{x}_{a2}(t) + l_1[y(t) - \hat{y}_a(t)] \\ \dot{\hat{x}}_{a2}(t) = u(t) + l_2[y(t) - \hat{y}_a(t)] \\ \dot{\hat{x}}_{a3}(t) = l_3[y(t) - \hat{y}_a(t)] \\ \hat{y}_a(t) = \hat{x}_{a1}(t) \\ \hat{d}_a(t) = \hat{x}_{a3}(t) \end{cases} \tag{9}$$

produces an estimate of the disturbance, $\hat{d}_a(t)$.

On the other hand, a GESO [5], [10] exactly estimates the disturbance, $d(t)$

$$\begin{cases} \dot{\hat{x}}_{g1}(t) = \hat{x}_{g2}(t) + \hat{x}_{g3}(t) + l_1[y(t) - \hat{y}_g(t)] \\ \dot{\hat{x}}_{g2}(t) = -\hat{x}_{g1}(t) - \hat{x}_{g2}(t) + u(t) + l_2[y(t) - \hat{y}_g(t)] \\ \dot{\hat{x}}_{g3}(t) = l_3[y(t) - \hat{y}_g(t)] \\ \hat{y}_g(t) = \hat{x}_{g1}(t) \\ \hat{d}_g(t) = \hat{x}_{g3}(t) \end{cases} \tag{10}$$

where $\hat{d}_g(t)$ is an estimate of $d(t)$ in (4).

B. Equivalent-Input-Disturbance Approach

Since only the control input in a control system can be used to deal with disturbances, the EID approach defines an EID, $d_e(t)$, on the control input channel that produces the same effect on the output as disturbances do [15], [25], and interprets Plant (4) as

$$\begin{cases} \dot{x}_{e1}(t) = x_{e2}(t) \\ \dot{x}_{e2}(t) = -x_{e1}(t) - x_{e2}(t) + u(t) + d_e(t) \\ y(t) = x_{e1}(t). \end{cases} \tag{11}$$

A state observer

$$\begin{cases} \dot{\hat{x}}_{e1}(t) = \hat{x}_{e2}(t) + l_1[y(t) - \hat{y}(t)] \\ \dot{\hat{x}}_{e2}(t) = -\hat{x}_{e1}(t) - \hat{x}_{e2}(t) + u_f(t) + l_2[y(t) - \hat{y}(t)] \\ \hat{y}_e(t) = \hat{x}_{e1}(t) \end{cases} \tag{12}$$

produces an EID estimate of the disturbance [15]

$$\hat{d}_e(t) = l_2[y(t) - \hat{y}_e(t)] + u_f(t) - u(t). \tag{13}$$

A low-pass filter $F(s)$ selects a frequency band for disturbance estimation

$$\tilde{D}_e(s) = F(s)\hat{D}_e(s). \tag{14}$$

If a first-order filter

$$F(s) = \frac{1}{Ts+1} \tag{15}$$

is used, then the resulting EID estimate is

$$\dot{\hat{d}}_e(t) = \frac{l_2}{T}[y(t) - \hat{y}_e(t)] \tag{16}$$

which has the same form as $\hat{x}_{a3}(t)$ in (9) does.

Note that the ESO method uses the minimum information of a plant (only the relative degree of a plant from the control input to the output is required) to carry out disturbance rejection. The configuration of a control system is the simplest. It is easy to apply the method to many actual systems. However, it requires that the zeros of a linear plant are all in the open left half-plane or that the zero dynamics of a nonlinear plant is stable. Moreover, since the difference between the dynamics of a plant and a series of integrators is lumped into the disturbance, extra control effort is needed to compensate for it. Let the order of the plant be n and the relative degree from the disturbance to the output be r. It also requires that the disturbance is $(n-r)$-times differentiable. The GESO method takes the structure of a plant into consideration and yields a disturbance estimate in (10) that is tighter than that given in (7).

A comparison between the mechanisms of the GESO and the EID methods for disturbance estimation shows that, while the GESO uses an extended state to skillfully produce a disturbance estimate, the EID tries to elegantly combine the state of an observer, a control input, and an output to derive an estimate of the EID.

Considering that the GESO and EID are the improvements of the ESO and DOB, respectively, we mainly compare these two methods in the rest of this paper to clarify the difference between these two types of methods.

Although both the GESO and EID methods make use of the dynamics of a plant by taking the structure of a plant into consideration and have a similar system structure, there are big differences between them. A comparison was carried out from the assumptions, stability, system design, control performance, and extensibility of these two methods in this study.

Remark 1: Even though all active-disturbance-rejection methods produce a compensation amount for disturbances on a control input channel, the thoughts are quite different. While the ESO and GESO try to produce the exact total disturbance, the DOB and EID methods focus on the effect of disturbances on the output. Since the purpose of control is to stabilize an output or ensure that an output tracks an input, the latter has a high affinity for control.

IV. Problem Formulation and Basic Characteristics of GESO and EID

Consider a plant

$$\begin{cases} \dot{x}(t) = Ax(t) + Bu(t) + B_d d(t) \\ y(t) = Cx(t) \end{cases} \tag{17}$$

where $x(t) \in \mathbb{R}^n$, $d(t) \in \mathbb{R}^{n_d}$, $u(t) \in \mathbb{R}^m$, and $y(t) \in \mathbb{R}^p$. Note that a disturbance is called a matched disturbance if $\text{rank}\{B\ B_d\} = \text{rank}\{B\}$; otherwise, it is called a mismatched one.

The following assumption is made about the plant.

Assumption 1: The system with (A, B, C) is controllable and observable.

Remark 2: In the literature on disturbance rejection, the system with (A, B, C) is usually assumed to satisfy Assumption 1. A plant needs to be observable for the GESO method because the method tries to estimate disturbances themselves. However, the EID approach does not require such a strong assumption because it focuses on the input-output relationship of a plant. Assumption 1 can be relaxed to one that the system with (A, B, C) is stabilizable and detectable. In fact, a system can be divided into four subsystems: controllable and observable, controllable but not observable, uncontrollable but observable, and neither controllable nor observable. Since both the controllable but not observable and neither controllable nor observable subsystems do not contribute to the system output, we just need them to be stable. The uncontrollable but observable subsystem can be taken to be a disturbance on the output of the controllable and observable subsystem. It is required to be stable to guarantee the stability of the subsystem. As a result, only the controllable and observable subsystem needs to be considered in the EID approach.

Note that only the control input can be used to reject disturbance. The problem considered in this study is stated as follows: *Produce a disturbance estimate for Plant (17) and use it to compensate for the disturbance.*

The plant is first described as

$$\begin{cases} \dot{x}_g(t) = A_g x_g(t) + B_g u(t) + E\dot{d}(t) \\ y(t) = C_g x_g(t) \\ x_{n+1}(t) = d(t) \end{cases} \tag{18}$$

for the design of a GESO-based control system (Fig. 1), where

$$\begin{cases} x_g(t) = \begin{bmatrix} x(t) \\ x_{n+1}(t) \end{bmatrix}, A_g = \begin{bmatrix} A & B_d \\ 0 & 0 \end{bmatrix}, B_g = \begin{bmatrix} B \\ 0 \end{bmatrix}, E = \begin{bmatrix} 0 \\ 1 \end{bmatrix} \\ C_g = \begin{bmatrix} C & 0 \end{bmatrix}. \end{cases} \tag{19}$$

Then, a GESO is built as

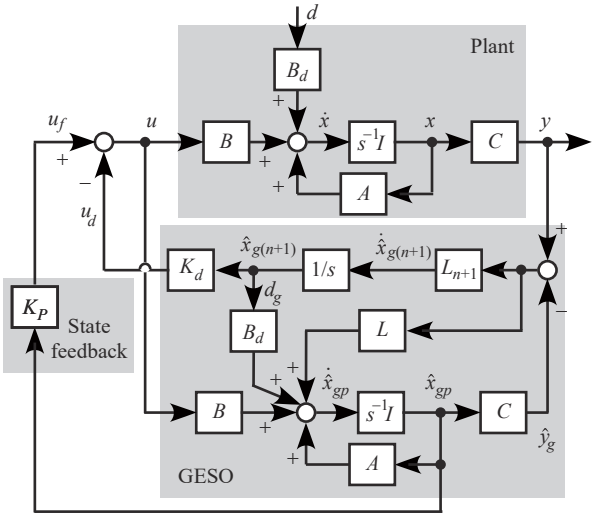

Fig. 1. GESO-based control system.

$$\begin{cases} \dot{\hat{x}}_g(t) = A_g\hat{x}_g(t) + B_g u(t) + L_g[y(t) - \hat{y}_g(t)] \\ \hat{y}_g(t) = C_g\hat{x}_g(t) \\ \hat{d}_g(t) = \hat{x}_{g(n+1)}(t) \end{cases} \tag{20}$$

where

$$\hat{x}_g(t) = \begin{bmatrix} \hat{x}_{gp}(t) \\ \hat{x}_{g(n+1)}(t) \end{bmatrix},\ L_g = \begin{bmatrix} L \\ L_{n+1} \end{bmatrix} \tag{21}$$

in which $\hat{x}_g(t)$ is the state of a GESO for disturbance estimation. An estimate of the disturbance, $\hat{d}_g(t)$, is incorporated into a state-feedback control law

$$\begin{cases} u(t) = u_f(t) - u_d(t) \\ u_f(t) = K_P\hat{x}_{gp}(t) \\ u_d(t) = K_d\hat{x}_{g(n+1)}(t) \end{cases} \tag{22}$$

where K_P is a state-feedback gain and K_d is a disturbance-compensation gain that is chosen to be

$$K_d = \left[C(A+BK_P)^{-1}B\right]^{-1}C(A+BK_P)^{-1}B_d \tag{23}$$

to match the direct-current (DC) gain.

The following assumptions are made for the GESO method [5], [10].

Assumption 2: $d(t)$ is bounded and a constant in the steady state, that is,

i) $\|d(t)\|_2 < \infty$;

ii) $\lim\limits_{t\to\infty} d(t) = \text{constant}$.

Assumption 3: The numbers of the inputs and outputs are the same and

$$\text{rank}\left\{C(A+BK_P)^{-1}B\right\} = \text{rank}\left\{C(A+BK_P)^{-1}[B, -B_d]\right\} \tag{24}$$

holds.

On the other hand, the EID approach first shows an equivalent expression of Plant (17)

$$\begin{cases} \dot{x}_e(t) = Ax_e(t) + Bu(t) + Bd_e(t) \\ y(t) = Cx_e(t). \end{cases} \tag{25}$$

Then, the combination of a state observer

$$\begin{cases} \dot{\hat{x}}_e(t) = A\hat{x}_e(t) + Bu_f(t) + L[y(t) - \hat{y}_e(t)] \\ \hat{y}_e(t) = C\hat{x}_e(t) \end{cases} \tag{26}$$

and the control input yields an EID estimate

$$\hat{d}_e(t) = B^+L[y(t) - \hat{y}_e(t)] + u_f(t) - u(t) \tag{27}$$

where

$$B^+ = \left(B^TB\right)^{-1}B^T \tag{28}$$

is the pseudo-inverse matrix of B. Filtering the estimate using a low-pass filter $F(s)$ yields the final estimate

$$\tilde{D}_e(s) = F(s)\hat{D}_e(s). \tag{29}$$

Combining the EID estimate in a state-feedback control law

$$u(t) = u_f(t) - \tilde{d}_e(t),\ u_f(t) = K_P\hat{x}_e(t) \tag{30}$$

gives the EID-based control-system configuration (Fig. 2).

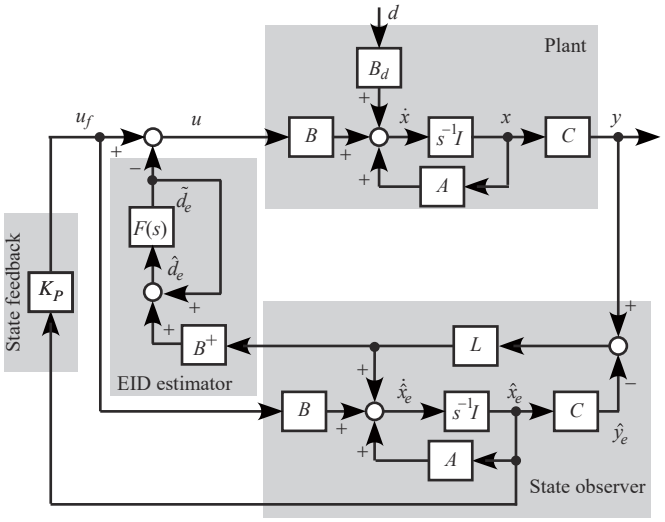

Fig. 2. EID-based control system.

The following assumption is made for the EID approach.

Assumption 4: The output due to the disturbance, $d(t)$, belongs to a set

$$\Phi = \{p_i(t)\sin(\omega_i t + \phi_i)\},\ i = 0, 1, \ldots, q \tag{31}$$

where $\omega_i\ (\geq 0)$ and ϕ_i are constants, $p_i(t)$ is a polynomial in time t, and q is a positive integer.

An actual control system easily satisfies Assumption 4. In fact, if an output produced by a disturbance belongs to Φ, then the learning-control method can be used to generate a corresponding control input in Φ. Thus, a feasible EID always exists. This strategy has widely been used to produce a control input for robot training [26].

A comparison between the GESO and the EID methods reveals the follows.

Assumptions on Disturbances: The GESO requires that B_d is known [see (23)], that is, a disturbance needs to be specified, but the EID does not need this information. Disturbances come from different sources. It may be difficult to find B_d in some systems. While the GESO tries to precisely estimate the disturbance itself, the EID produces an EID estimate that has the same effect on the output as the disturbance does. The

GESO requires that disturbances satisfy Assumption 2. However, ii) in the assumption is difficult to be satisfied except for a step signal. For example, a sinusoidal disturbance is not a constant as t tends to infinity. Thus, this condition is strict for control practice. On the other hand, since a physical plant usually has a low-pass characteristic, high-frequency components in a disturbance give little influence on the output. Assumption 4 is usually satisfied. This lowers the barrier between the theory and its application.

It is also clear from (20) that the GESO cannot directly handle an output disturbance, while the EID does.

Applicable Plant: While the EID can be applied to a non-square plant (the numbers of the inputs and outputs are not the same), Assumption 3, which ensures the existence of K_d, restricts the GESO to a square plant (the numbers of the inputs and outputs are the same). Many actual plants are non-square ones, for example, a building usually has more outputs than its control inputs. To solve this problem, the GESO needs to redefine outputs for a non-square plant to build a new square one [5].

V. Stability Analysis and System Design

The basic construction of GESO- and EID-based control systems is the combination of a state observer and a feedback-control system. The observer and the feedback-control law can be designed separately if stability is the only concern. Thus, Separation Theorem is used to derive stability conditions for both GESO- and EID-based control systems.

First, an error system is derived from (18) and (20)

$$\begin{cases} \Delta\dot{x}_g(t) = A_{gL}\Delta x_g(t) - E\dot{d}(t) \\ \Delta x_g(t) = \hat{x}_g(t) - x_g(t) = \begin{bmatrix} \hat{x}_{gp}(t) - x(t) \\ \hat{d}_g(t) - d(t) \end{bmatrix} = \begin{bmatrix} \Delta x_{gp}(t) \\ \Delta d_g(t) \end{bmatrix} \\ A_{gL} = A_g - L_g C_g \end{cases} \tag{32}$$

to analyze the stability of the GESO-based control system.

Combining (17), (22), and (32) yields

$$\begin{bmatrix} \dot{x}(t) \\ \Delta\dot{x}_g(t) \end{bmatrix} = \begin{bmatrix} A + BK_P & B\bar{K} \\ 0 & A_{gL} \end{bmatrix} \begin{bmatrix} x(t) \\ \Delta x_g(t) \end{bmatrix} + \begin{bmatrix} 0 & \bar{B}_d \\ -E & 0 \end{bmatrix} \begin{bmatrix} \dot{d}(t) \\ d(t) \end{bmatrix} \tag{33}$$

where

$$\bar{K} = [K_P \quad -K_d], \quad \bar{B}_d = B_d - BK_d. \tag{34}$$

The following lemma presents stability conditions for the GESO-based control system.

Lemma 1 ([5]): The GESO-based control system is bounded-input bounded-output (BIBO) stable if

i) Both $d(t)$ and $\dot{d}(t)$ are bounded;

ii) The state-feedback gain, K_P, in (22) is selected such that $(A + BK_P)$ is Hurwitz;

iii) The observer gain, L_g, in (21) is selected such that A_{gL} in (32) is Hurwitz.

The following lemma presents conditions for disturbance rejection for the GESO method.

Lemma 2 (Theorem 6.2 in [10]): The control law (22) rejects the disturbance in (17) on the output in the steady state if

i) The system is stable (that is, Lemma 1 holds);

ii) $C(A + BK_P)^{-1}B$ in (23) is invertible; and

iii) Assumptions 2 and 3 hold.

To design a GESO-based control system, not only $(A + BK_P)$ and A_{gL} in (33) are required to be Hurwitz, but also the eigenvalues of A_{gL} are needed to be selected to ensure that the convergent speed of the GESO is faster than that of the closed-loop system.

Choosing all the poles of the GESO to be the same is a simple design strategy for A_{gL} [7]. For example, if the bandwidth for state estimation is chosen to be ω_g, then the characteristic polynomial of the observer is

$$|sI - A_{gL}| = (s + \omega_g)^{n+1}. \tag{35}$$

On the other hand, the stability of the EID control system is analyzed for $d(t) = 0$.

Letting

$$\Delta x_e(t) = \hat{x}_e(t) - x(t) \tag{36}$$

and combining (17) and (26) give

$$\Delta\dot{x}_e(t) = (A - LC)\Delta x_e(t) + B[u_f(t) - u(t)]. \tag{37}$$

Redrawing Fig. 2 using the relationships of (17), (27), (29), and (30) yields Fig. 3, in which the transfer function from $\tilde{d}_e(t)$ to $\hat{d}_e(t)$ is

$$\begin{aligned} G(s) &= I - B^+LC[sI - (A - LC)]^{-1}B \\ &= B^+(sI - A)[sI - (A - LC)]^{-1}B. \end{aligned} \tag{38}$$

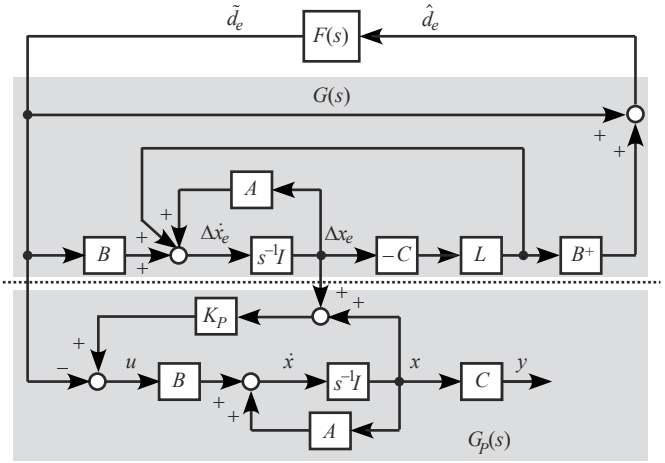

Fig. 3. Derivation of stability conditions for EID-based control system.

Observation of Fig. 3 yields the following stability conditions for the EID-based control system.

Lemma 3 ([15]): The EID-based control system is stable if the following conditions hold:

i) The state-feedback gain, K_P, in (30) is selected such that $(A + BK_P)$ is Hurwitz;

ii) The observer gain, L, in (26) is selected such that $(A - LC)$ is Hurwitz;

iii)

$$\|GF\|_\infty < 1 \tag{39}$$

where $F(s)$ is the low-pass filter used in (29).

A comparison between Lemmas 1 and 3 shows that, while i)

in Lemma 3 is exactly ii) in Lemma 1, ii) and iii) in Lemma 3 correspond to iii) in Lemma 1. Since iii) in Lemma 3 is derived from the small-gain theorem, it might be conservative. Bringing a scaling factor for the H_∞ problem in (39) reduces the conservativeness of the condition [27].

Note that using (35) to design A_{gL} for the GESO may result in an unstable state observer $(A-LC, B, C)$, that is, the internal stability of the system is not guaranteed. This may cause input saturation [28].

If a plant with (A, B, C) is a minimum-phase one, then the concept of perfect regulation ensures that

$$\lim_{\rho\to\infty}[sI-(A-L(\rho)C)]^{-1}B=0 \tag{40}$$

holds for a parameterized gain of the state observer $L(\rho)$ [15].

Equation (40) provides a way to find an observer gain that satisfies Condition iii) in Lemma 3. On the other hand, since (40) does not hold for a nonminimum-phase plant, a linear-matrix-inequality-based method, which combines the reduced-order H_∞ control and the cone complementarity linearization method, was presented in [29] instead.

A comparison of system design between the GESO and EID methods reveals the following.

Stability and System Design: The design method (35) for a GESO-based control system is simple and easy to use. Thus, it is widely used in control engineering practice. On the other hand, a multiple pole is sensitive to parameter changes [30]. Note that the perfect-regulation-based design method for an EID-based control system [15] is intuitive because a design process can be carried out using Bode plots. However, it may result in high gains that may cause a peaking phenomenon and may amplify measurement noise.

The transfer functions from an actual disturbance to an output for the GESO and EID are important to evaluate disturbance-rejection performance. They are calculated as following.

First, for the GESO method, rewrite (32) as

$$\begin{cases}\Delta\dot{x}_{gp}(t)=(A-LC)\Delta x_{gp}(t)+B_d\Delta d_g(t)\\ \hat{x}_{g(n+1)}(t)=-L_{n+1}C\Delta x_{gp}(t).\end{cases} \tag{41}$$

Note that

$$\begin{aligned}u(t)&=K_P[x(t)+\Delta x_{gp}(t)]-K_d\hat{x}_{g(n+1)}\\&=K_Px(t)+K_P\Delta x_{gp}(t)-K_d\hat{x}_{g(n+1)}.\end{aligned} \tag{42}$$

Combining (17), (41), and (42) yields the block diagram from $d(t)$ to $y(t)$ (Fig. 4). Rearranging the blocks gives the transfer function (Fig. 5)

$$G_{yd}^{GESO}(s)=G_{SF}(s)G^{GESO}(s) \tag{43}$$

where

$$\begin{cases}G_{SF}(s)=C[sI-(A+BK_P)]^{-1}\\ G^{GESO}(s)=B_d+BG^G(s)G_{OB}^G(s)\end{cases} \tag{44}$$

where

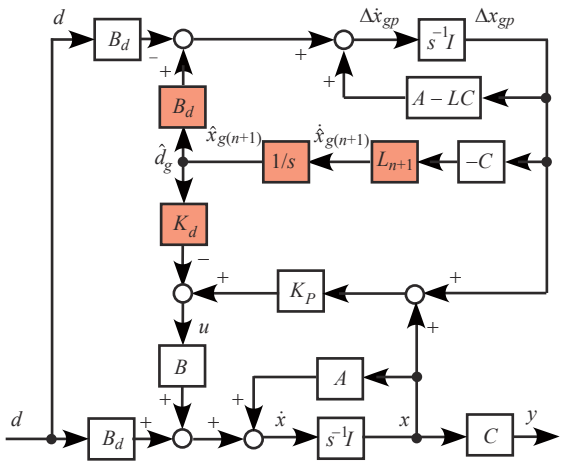

Fig. 4. Block diagram from disturbance to output for GESO.

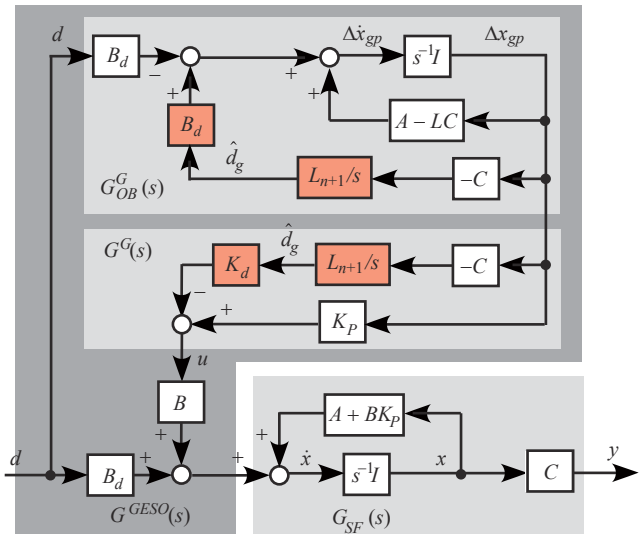

Fig. 5. Rearrangement of Fig. 4.

$$\begin{cases}G^G(s)=K_P+K_dL_{n+1}C/s\\ G_{OB}^G(s)=-s[sI+M(s)B_dL_{n+1}C]^{-1}M(s)B_d\\ M(s)=[sI-(A-LC)]^{-1}.\end{cases} \tag{45}$$

Thus, if

$$G^{GESO}(j\omega)\approx 0,\ \omega\in[0,\ \omega_e] \tag{46}$$

holds, the GESO method can reject both matched and mismatched disturbances.

Let

$$F^G(s)=\frac{1}{\frac{1}{L_{n+1}}s+1}. \tag{47}$$

A large enough L_{n+1} provides

$$F^G(j\omega)\approx 1,\ \forall\omega\in[0,\ \omega_e]. \tag{48}$$

A simple calculation yields

$$G^{GESO}(s)=G_1^{GESO}(s)+G_2^{GESO}(s) \tag{49}$$

where

$$\begin{cases} G_1^{GESO}(s) = [1 - F^G(s)][sI - (A + BK_P - LC)] \\ \qquad \times \{[1 - F^G(s)]M^{-1}(s) + F^G(s)B_dC\}^{-1}B_d \\ G_2^{GESO}(s) = F^G(s)(B_d - BK_d)C \\ \qquad \times \{[1 - F^G(s)]M^{-1}(s) + F^G(s)B_dC\}^{-1}B_d. \end{cases} \tag{50}$$

Next, for the EID approach, combining (17), (25), and (30) yields

$$\Delta\dot{x}_e(t) = (A - LC)\Delta x_e(t) + B\tilde{d}_e(t) - B_d d(t). \tag{51}$$

Substituting (36) into (30) yields

$$\begin{aligned} u(t) &= K_P[x(t) + \Delta x_e(t)] - \tilde{d}_e(t) \\ &= K_P x(t) + K_P \Delta x_e(t) - \tilde{d}_e(t). \end{aligned} \tag{52}$$

Combining (27) and (30) yields

$$\hat{d}_e(t) = -B^+LC\Delta x_e(t) + \tilde{d}_e(t). \tag{53}$$

The relationships (17), (51), (52), and (53) provide the block diagram from $d(t)$ to $y(t)$ (Fig. 6). Rearranging the blocks gives Fig. 7 and the transfer function is

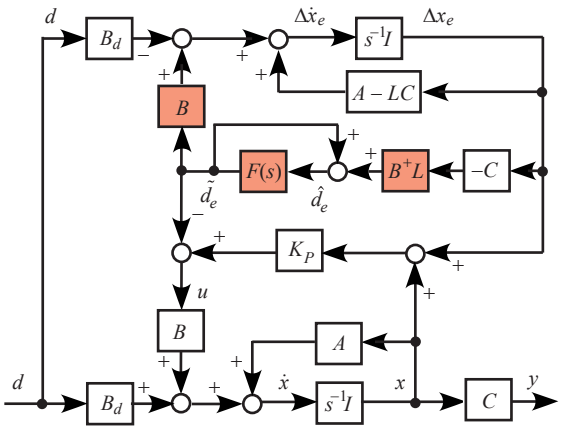

Fig. 6. Block diagram from disturbance to output for EID.

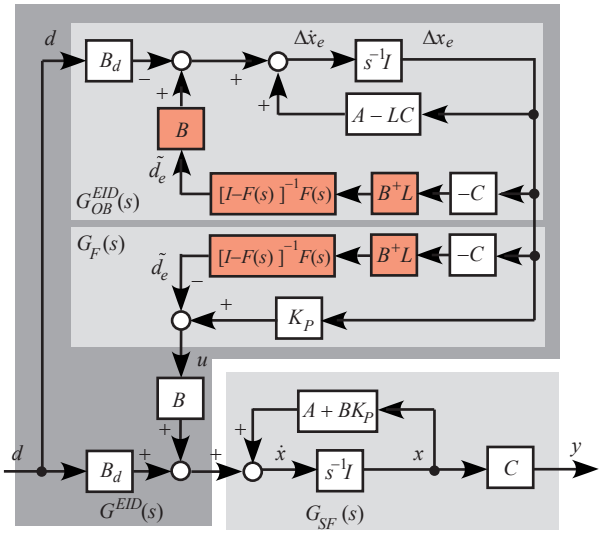

Fig. 7. Rearrangement of Fig. 6.

$$G_{yd}^{EID}(s) = G_{SF}(s)G^{EID}(s) \tag{54}$$

where $G_{SF}(s)$ is shown in (44) and $G^{EID}(s)$ is the part related to the EID that is given by

$$\begin{cases} G^{EID}(s) = B_d + BG_F(s)G_{OB}^E(s) \\ G_F(s) = K_P + [I - F(s)]^{-1}F(s)B^+LC \\ G_{OB}^E(s) = -\{I + M(s)B[I - F(s)]^{-1}F(s)B^+LC\}^{-1} \\ \qquad \times M(s)B_d \end{cases} \tag{55}$$

where $M(s)$ is given in (45).

Choosing

$$F(s) = F_1(s)I,\ F_1(j\omega) \approx 1,\ \forall\omega \in [0,\ \omega_e] \tag{56}$$

gives

$$\begin{aligned} G^{EID}(s) &= [1 - F_1(s)][sI - (A + BK_P - LC)] \\ &\quad \times \left\{[1 - F_1(s)]M^{-1}(s) + F_1(s)BB^+LC\right\}^{-1} B_d. \end{aligned} \tag{57}$$

The selection of (56) ensures that the EID approach rejects both matched and mismatched disturbances.

A comparison of $G^{GESO}(s)$ [in (49) and (50)] and $G^{EID}(s)$ [in (57)] shows that $G^{GESO}(s)$ has two terms and the first term, $G_1^{GESO}(s)$, corresponds to $G^{EID}(s)$, which has a small gain in a selected disturbance-rejection frequency band. The difference in the disturbance-rejection performance between these two methods is caused by the term $G_2^{GESO}(s)$ in (49).

Remark 3: Yu *et al.* introduced a new item K_e to ease system design in [31], which corresponds to B^+L in the EID approach (Figs. 6 and 7).

A comparison of the disturbance rejection methods between the GESO and EID reveals the following:

Disturbance Estimation and Compensation: As shown in (20) and (22), the GESO estimates the disturbance itself but adds an estimate on the control input channel. Thus, there is a gap between the estimation and its use. The method uses a gain K_d in (23) to transfer the estimate of a mismatched disturbance to the control input channel. Since the gain is fitted for a prescribed frequency (usually for $\omega = 0$), high disturbance-rejection performance is expected around such a frequency. On the other hand, as shown in [25], the EID approach estimates the EID directly. It almost completely compensates for the disturbance if the low-pass filter $F(s)$ satisfies (56). Moreover, embedding a gain in the filter makes it possible to further elaborate disturbance-rejection characteristics [32], [33]. Thus, the EID approach is easy and flexible in adjusting disturbance-rejection performance.

VI. Numerical Verification

Plant (4) is used as an example to verify and compare disturbance-rejection performance for the two methods. The parameters in (17) are

$$A = \begin{bmatrix} 0 & 1 \\ -1 & -1 \end{bmatrix},\ B = \begin{bmatrix} 0 \\ 1 \end{bmatrix},\ B_{du} = \begin{bmatrix} 1 \\ 0 \end{bmatrix},\ B_{dm} = B,\ C = \begin{bmatrix} 1 \\ 0 \end{bmatrix}^T \tag{58}$$

where B_{du} and B_{dm} are for a mismatched and a matched disturbance, respectively.

Note that the cutoff angular frequency of the plant is 1 rad/s. The disturbance (Fig. 8)

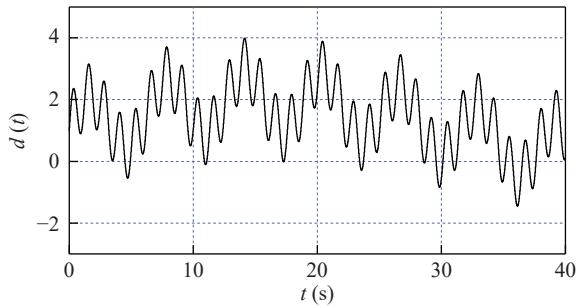

Fig. 8. Disturbance (59).

$$d(t) = 1 + \sin 0.1t + \sin t + \sin 5t \tag{59}$$

was used to compare the two methods to verify the ability of disturbance estimation and compensation. It contains a DC component, a component of 1 rad/s, a low-frequency component (0.1 rad/s), and a high-frequency component (5 rad/s).

Choosing

$$Q_k = 100 \times C^T C,\ R_k = 1 \tag{60}$$

and optimizing

$$J_k = \int_0^\infty \left\{ x^T(t) Q_k x(t) + u^T(t) R_k u(t) \right\} dt \tag{61}$$

yielded

$$K_P = [-9.0499 \quad -3.3703],\ K_d = 4.3703. \tag{62}$$

Since the bandwidth of the state-feedback control system $(A + BK_P, B, C)$ is 3.25 rad/s, we chose the cutoff angular frequency of the GESO to be about five times larger than it

$$\omega_g = 16 \text{ rad/s}. \tag{63}$$

This gives the characteristic polynomial of the GESO, (35), and its gain

$$L_g = [47 \quad -3376 \quad 4096]^T. \tag{64}$$

To carry out a comparison between the GESO and the EID methods, we chose

$$\rho = 10^6,\ Q_L = \text{diag}\{1, 260\},\ R_L = 1 \tag{65}$$

for the EID. Solving the following algebraic Riccati equation:

$$AP + PA^T + \rho Q_L - PC^T R_L^{-1} CP = 0 \tag{66}$$

yielded

$$L = [1015 \quad 15\,139]^T \tag{67}$$

which has the same cutoff angular frequency, ω_g, as the ESGO does. The gain of the state feedback, K_P, was set to be (62). The first-order low-pass filter (15) was used and the time constant was chosen to be

$$T = 0.0625 \text{ s} \tag{68}$$

that is, the cutoff angular frequency of the filter is also ω_g in (63).

Note that the poles of the GESO ($|sI - A_{gL}| = 0$) are a cube root at -16 [refer to (63)]. It results in the poles of the state observer $[|sI - (A - LC)| = 0]$ being -86.48 and 38.48. One of them is unstable. This may not be acceptable for some control applications. In this case, ω_g should be selected as small as 3 to ensure that $(A - LC)$ is Hurwitz. In contrast, the poles of the observer for the EID approach are always stable (they are -16.16 and -999.9).

Simulation results for the matched disturbance ($B_d = B_{dm}$) (Fig. 9) show that the control inputs of these methods are at the same level, but the absolute peak value of the output for the EID is only as small as 2% of that for the GESO. Simulation results for the mismatched disturbance ($B_d = B_{du}$) (Fig. 10) show that, while the control input for the GESO is more than 3 times larger than that for the EID, the output for the GESO is more than 60 times larger than that for the EID.

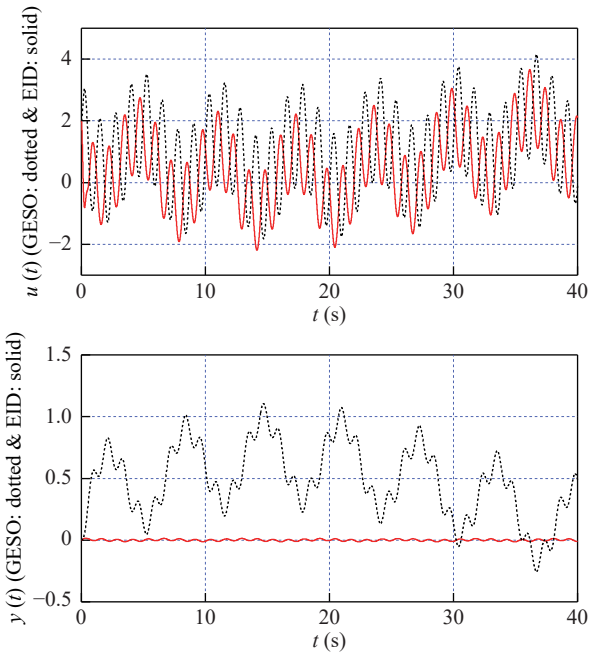

Fig. 9. Simulation results for matched disturbance ($B_d = B_{dm}$).

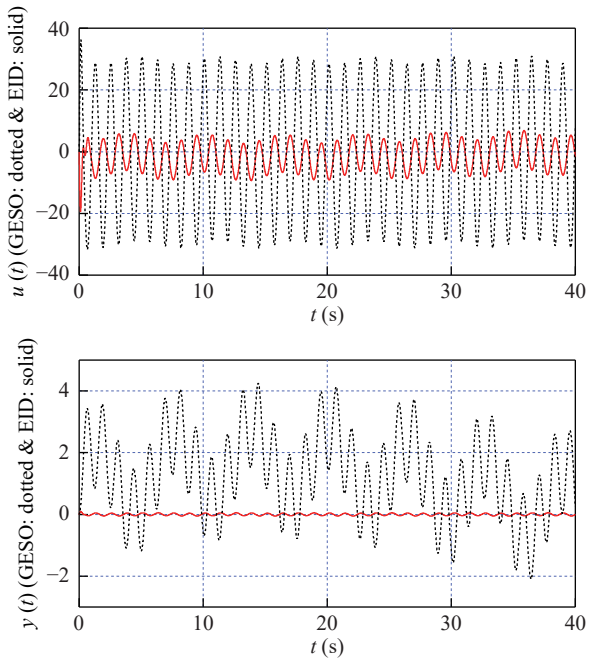

Fig. 10. Simulation results for mismatched disturbance ($B_d = B_{du}$).

Choose $\gamma_{LQG} = \gamma_{peak} = 0.01$, $\lambda = 1$, $T_s = 0$, and $T_f = 40$ s. The disturbance-rejection performance (3) was 16.052 for the GESO and 1.440 for the EID for the matched disturbance, and was 321.859 for the GESO and 9.231 for the EID for the mismatched disturbance. The spectra of the outputs in Figs. 9 and 10 also show that those spectra at the frequencies 0.1, 1, and 5 rad/s are much smaller for the EID than for the GESO (Fig. 11). These statistics show the superiority of the EID approach over the GESO method.

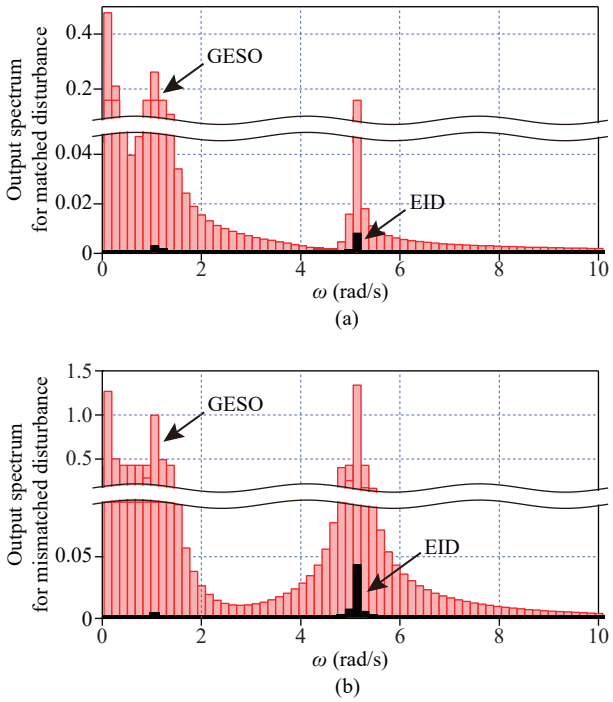

Fig. 11. Spectra of outputs for matched and mismatched disturbance: (a) Matched disturbance ($B_d = B_{dm}$); (b) Mismatched disturbance ($B_d = B_{du}$).

VII. Limitation and Extensibility

The estimators used for disturbance estimation are mainly first-order systems for both GESO and EID methods. Attempts have been made to use high-order estimators to improve disturbance-rejection performance.

The GESO method guarantees the convergence of disturbance estimation only when a disturbance satisfies Assumption 2. This assumption is strict because many disturbances are not constants in the steady state. A new state observer was derived to improve the precision of disturbance estimation. Unlike the GESO that uses only one state component to estimate a disturbance, a new GESO has multiple state components to yield a satisfactory estimate for a time-varying disturbance [34]. However, an estimator containing m state components requires that a disturbance is m-times continlinebreak hyphen="true"/>uously differentiable.

In contrast, the EID approach pays attention to disturbance-rejection performance. A method was presented in [35] to add a stable zero in the low-pass filter in an EID estimator to enable phase-lead compensation that enlarges the range of parameter selection for disturbance compensation. This strategy also improves noise-suppression performance [36].

Another attempt was made to embed an internal model of a disturbance in a GESO [37] and in the low-pass filter in an EID estimator [38] to completely compensate for a disturbance in the steady state. This strategy greatly increases the steady-state disturbance-rejection performance.

Compensation for Nonlinearities: Since nonlinearities, uncertainties, and disturbances can be lumped as a total disturbance [39], that is, such a term $f(x(t), d_s(t), t)$ is taken to be $d(t)$ in (17), it is possible to compensate for it using the GESO or EID methods. The stability of a GESO-based control system was proved for $d(t) = f(d_s(t), t)$ in [10], and the stability and an upper bound of an EID-based control system were proved for state-dependent nonlinearities based on the concept of globally uniformly ultimately bounded [40], [41]. While a Lipschitz condition is required for the GESO method for nonlinearity compensation [42], it is not necessary for the EID approach because the use of the estimated state in the reconstruction of the nonlinearity ensures the convergence of the observation error [43]. This is a big advantage of the EID approach over the GESO method.

Augmentability: Since both GESO and EID estimate a disturbance, they can be used to carry out fault diagnoses. Note that, while the GESO method estimates a fault itself, the EID approach estimates the EID, that is, the damage to the system caused by a fault. Thus, combining these two methods for fault diagnosis not only obtains precise information about a fault (an estimate given by the GESO) but also provides the impact of a fault on the system (an estimate given by the EID). This combination may provide a new method of a comprehensive fault diagnosis.

VIII. Conclusion

Disturbance rejection is important in control engineering practice. Control methods have been proposed to deal with this problem from various viewpoints. Among them, the methods of actively estimating and rejecting disturbances are simple and effective, and thus are used in mechatronic and other control systems to obtain high control performance. This study carried out an inside comparison between two active disturbance-control methods: the GESO and EID. We compared them from the aspects of the assumptions, the system configurations, the stability conditions, the system design, the disturbance-rejection mechanisms and performance, and the extensibility.

While the GESO has been widely used, many engineers do not have a firm belief whether or not the use of the method is suitable because disturbances in control practice usually do not meet Assumption 2. On the other hand, the EID approach is a method that has a realistic assumption on disturbances, thus providing us confidence in practice. Regarding disturbance-rejection performance, the EID approach directly estimates a signal on the control input channel, while the GESO method first estimates a disturbance itself and then converts it into a signal on the control input channel. Note that the conversion only matches the compensation gain for a prescribed frequency. On the other hand, the disturbance-rejection per-

formance for the EID approach is guaranteed by the selection of the low-pass filter in the EID estimator. This is a big advantage of the EID over the GESO. A numerical example verified the difference in disturbance-rejection performance between these two methods.

Some noticeable issues for active disturbance rejection, including the GESO and EID, are how to further improve disturbance-rejection performance [44]; how to use a reduced-order observer for disturbance estimation [45], [46]; how to improve noise-suppression performance [36], [47]; how to reduce the effect of peaking phenomena [48]; how to design such a system for a time-delay system [49]; and how to alleviate restrictions and limitations in a system, for example, input saturation [50]. Some attempts have been carried out on them, and have received a great deal of attention.

REFERENCES

[1] M. Ruderman, M. Iwasaki, and W.-H. Chen, "Motion-control techniques of today and tomorrow," *IEEE Ind. Electron. Mag.*, vol. 14, no. 1, pp. 41–55, 2020.

[2] J. Han, "From PID to active disturbance rejection control," *IEEE Trans. Ind. Electron.*, vol. 56, no. 3, pp. 900–906, 2009.

[3] Q. Zhang and Z. Gao, "Active disturbance rejection control: Some recent experimental and industrial case studies," *Control Theory Tech.*, vol. 16, no. 4, pp. 301–313, 2018.

[4] H. Sira-Ramírez, E. W. Zurita-Bustamante, and C. Huang, "Equivalence among flat filters, dirty derivative-based PID controllers, ADRC, and integral reconstructor-based sliding mode control," *IEEE Trans. Control Syst. Technol.*, vol. 28, no. 9, pp. 1696–1710, 2020.

[5] S. Li, J. Yang, W.-H. Chen, and X. Chen, "Generalized extended state observer based control for systems with mismatched uncertainties," *IEEE Trans. Ind. Electron.*, vol. 59, no. 12, pp. 4792–4802, 2012.

[6] A. A. Godbole, J. Kolhe, and S. E. Talole, "Performance analysis of generalized extended state observer in tackling sinusoidal disturbances," *IEEE Trans. Control Syst. Technol.*, vol. 21, no. 6, pp. 2212–2223, 2013.

[7] Y. Huang and W. Xue, "Active disturbance rejection control: Methodology and theoretical analysis," *ISA Trans.*, vol. 53, pp. 963–976, 2014.

[8] H. Feng and B.-Z. Guo, "Active disturbance rejection control: Old and new results," *Annu. Rev. Control*, vol. 44, pp. 238–248, 2017.

[9] H. Sira-Ramírez, A. Luviano-Juárez, M. Ramírez-Neria, and E. W. Zurita-Bustamante, *Active Disturbance Rejection Control of Dynamic Systems: A Flatness Based Approach*, Butterworth-Heinemann, UK, 2017.

[10] S. Li, J. Yang, W.-H. Chen, and X. Chen, *Disturbance Observer-Based Control: Methods and Applications*, CRC Press, 2013.

[11] S. E. Talole, "Active disturbance rejection control: Applications in aerospace," *Control Theory Technol.*, vol. 16, pp. 314–323, 2018.

[12] Q. Lu, D. Zhang, W. Ye, J. Fan, S. Liu, and C.-Y. Su, "Targeting posture control with dynamic obstacle avoidance of constrained uncertain wheeled mobile robots including unknown skidding and slipping," *IEEE Trans. Syst. Man Cybern.: Syst.*, vol. 51, no. 11, pp. 6650–6659, 2021.

[13] A. Sabanovic and K. Ohnishi, *Motion Control Systems*, John Wiley & Sons (Asia) Pte Ltd, Singapore, 2011.

[14] E. Sariyildiz, R. Oboe, and K. Ohnishi, "Disturbance observer-based robust control and its applications: 35th anniversary overview," *IEEE Trans. Ind. Electron.*, vol. 67, no. 3, pp. 2042–2053, 2020.

[15] J. She, M. Fang, Y. Ohyama, H. Hashimoto, and M. Wu, "Improving disturbance-rejection performance based on an equivalent-input-disturbance approach," *IEEE Trans. Ind. Electron.*, vol. 55, no. 1, pp. 380–389, 2008.

[16] W.-H. Chen, J. Yang, L. Guo, and S. Li, "Disturbance-observer-based control and related methods—An overview," *IEEE Trans. Ind. Electron.*, vol. 63, no. 2, pp. 1083–1095, 2015.

[17] T. E. Marlin, *Process Control: Designing Processes and Control Systems for Dynamic Performance*, McGraw-Hill, 2nd Ed., 2014.

[18] B. B. Alagoz, F. N. Deniz, C. Keles, and N. Tan, "Disturbance rejection performance analysis of closed loop control systems by reference to disturbance ratio," *ISA Trans.*, vol. 55, pp. 63–71, 2015.

[19] W. Xue and Y. Huang, "Performance analysis of active disturbance rejection tracking control for a class of uncertain LTI systems," *ISA Trans.*, vol. 58, pp. 133–154, 2015.

[20] B. Huang and S. L. Shah, *Performance Assessment of Control Loops: Theory and Applications*, Springer, 1999.

[21] P. D. Domański, *Control Performance Assessment: Theoretical Analyses and Industrial Practice*, Springer, 2020.

[22] M. Jelali, *Control Performance Management in Industrial Automation: Assessment, Diagnosis and Improvement of Control Loop Performance*, Springer, 2013.

[23] M. Farza, A. Ragoubi, S. Hadj Saïd, and M. M'Saad, "Improved high gain observer design for a class of disturbed nonlinear systems," *Nonlinear Dyn.*, vol. 106, pp. 631–655, 2021.

[24] J. Han, *Active Disturbance Rejection Control Technique—The Technique for Estimating and Compensating the Uncertainties*, National Defense Industry Press, Beijing, 2013 (in Chinese).

[25] J. She, X. Xin, and Y. Pan, "Equivalent-input-disturbance approach—Analysis and application to disturbance rejection in dual-stage feed drive control system," *IEEE/ASME Trans. Mechatron.*, vol. 16, no. 2, pp. 330–340, 2011.

[26] C. H. Park, J. H. Kyung, D. I. Park, K. T. Park, D. H. Kim, and D. G. Gweon, "Direct teaching algorithm for a manipulator in a constraint condition using the teaching force shaping method," *Adv. Robot.*, vol. 24, pp. 1365–1384, 2010.

[27] K.-Z. Liu and Y. Yao, *Robust Control: Theory and Applications*, John Wiley & Sons, 2016.

[28] J. C. Doyle, R. S. Smith, and D. F. Enns, "Control of plants with input saturation nonlinearities," in *Proc. Am. Control Conf.*, pp. 1034–1039, 1987.

[29] J. She, X. Xin, and Y. Ohyama, "Estimation of equivalent input disturbance improves vehicular steering control," *IEEE Trans. Veh. Technol.*, vol. 56, no. 6, pp. 3722–3731, 2007.

[30] C. E. Maley, "The effect of parameters on the roots of an equation system," *Comput. J.*, vol. 4, no. 1, pp. 62–63, 1961.

[31] P. Yu, K.-Z. Liu, J. She, M. Wu, and Y. Nakanishi, "Robust disturbance rejection for repetitive control systems with time-varying nonlinearities," *Int. J. Robust Nonlinear Control*, vol. 29, pp. 1597–1612, 2018.

[32] K. Miyamoto, J. She, J. Imani, X. Xin, and D. Sato, "Equivalent-input-disturbance approach to active structural control for seismically excited buildings," *Eng. Struct.*, vol. 125, pp. 392–399, 2016.

[33] P. Yu, M. Wu, J. She, K.-Z. Liu, and Y. Nakanishi, "Robust tracking and disturbance rejection for linear uncertain system with unknown state delay and disturbance," *IEEE/ASME Trans. Mechatron.*, vol. 23, no. 3, pp. 1445–1455, 2018.

[34] R. Madoński and Herman, "Survey on methods of increasing the efficiency of extended state disturbance observers," *ISA Trans.*, vol. 56, pp. 18–27, 2015.

[35] Y. Du, W. Cao, J. She, M. Wu, M. Fang, and S. Kawata, "Disturbance rejection and control system design using improved equivalent input disturbance approach," *IEEE Trans. Ind. Electron.*, vol. 67, no. 4, pp. 3013–3023, 2020.

[36] Y. Du, W. Cao, J. She, M. Wu, M. Fang, and S. Kawata, "Disturbance rejection and robustness of improved equivalent-input-disturbance-based system," *IEEE Trans. Cybern.*, vol. 52, no. 8, pp. 8537–8546, 2022

[37] B. Guo, S. Bacha, M. Alamir, A. Hably, and C. Boudinet, "Generalized integrator-extended state observer with applications to grid-connected converters in the presence of disturbances," *IEEE Trans. Control Syst. Technol.*, vol. 29, no. 2, pp. 744–755, 2021.

[38] Q. Mei, J. She, Z.-T. Liu, and M. Wu, "Estimation and compensation of periodic disturbance using internal-model-based equivalent-input-disturbance approach," *Sci. China Inf. Sci.*, vol. 65, no. 8, pp. 1182205: 1–14, 2022.

[39] S. Chen, W. Bai, Y. Hu, Y. Huang, and Z. Gao, "On the conceptualization of total disturbance and its profound implications," *Sci. China Inf. Sci.*, vol. 63, pp. 129201: 1–3, 2020.

[40] F. Gao, M. Wu, J. She, and W. Cao, "Disturbance rejection in nonlinear systems based on equivalent-input-disturbance approach," *Appl. Math. Comput.*, vol. 282, pp. 244–253, 2016.

[41] L. Ouyang, M. Wu, and J. She, "Estimation of and compensation for unknown input nonlinearities using equivalent-input-disturbance approach," *Nonlinear Dyn.*, vol. 88, no. 3, pp. 2161–2170, 2017.

[42] G. Tian, and Z. Gao, "From Poncelet's invariance principle to active disturbance rejection," in *Proc. Am. Control Conf.*, pp. 2451–2457, 2009, St. Louis, MO, USA

[43] X. Yin, J. She, M. Wu, D. Sato, and K. Hirota, "Disturbance rejection and performance analysis for nonlinear systems based on nonlinear equivalent-input-disturbance approach," *Nonlinear Dyn.*, vol. 100, no. 4, pp. 3497–3511, 2020.

[44] Z. Wang, J. She, Z.-T. Liu, and M. Wu, "Modified equivalent-input-disturbance approach to improving disturbance-rejection performance," *IEEE Trans. Ind. Electron.*, vol. 69, no. 1, pp. 673–683, 2022.

[45] J. Sun, J. Yang, and S. Li, "Reduced-order GPIO based dynamic event-triggered tracking control of a networked one-DOF link manipulator without velocity measurement," *IEEE/CAA J. Autom. Sinica*, vol. 7, no. 3, pp. 725–734, 2020.

[46] K. Miyamoto, J. She, S. Nakano, D. Sato, and Y. Chen, "Active structural control of base-isolated building using equivalent-input-disturbance approach with reduced-order state observer," *J. Dyn. Sys., Meas., Control*, vol. 144, no. 9, pp. 091006: 1–14, 2022.

[47] T. He and Z. Wu, "Iterative learning disturbance observer based attitude stabilization of flexible spacecraft subject to complex disturbances and measurement noises," *IEEE/CAA J. Autom. Sinica*, vol. 8, no. 9, pp. 1576–1587, 2021.

[48] D. Astolfi, L. Marconi, L. Praly, and A. R. Teel, "Low-power peaking-free high-gain observers," *Automatica*, vol. 98, pp. 169–179, 2018.

[49] Q. Wu, L. Yu, Y.-W. Wang, and W.-A. Zhang, "LESO-based position synchronization control for networked multi-axis servo systems with time-varying delay," *IEEE/CAA J. Autom. Sinica*, vol. 7, no. 4, pp. 1116–1122, 2020.

[50] X. Song, W. Xue, and Y. Zhao, "Control design for maximal capability of disturbance rejection under general control input saturation," *J. Franklin Inst.*, vol. 358, pp. 9771–9793, 2021.

Jinhua She (Fellow, IEEE) received the B.S. degree from Central South University in 1983, and the M.S. and Ph.D. degrees from Tokyo Institute of Technology, Japan, in 1990 and 1993, respectively, all in engineering.

In 1993, he joined the School of Engineering, Tokyo University of Technology, where he is currently a Professor. His research interests include the application of control theory, repetitive control, process control, m-learning, and assistive robotics.

Dr. She is a Member of the Chinese Association of Automation (CAA), the Society of Instrument and Control Engineers (SICE), Institute of Electrical Engineers of Japan (IEEJ), the Japan Society of Mechanical Engineers (JSME), Architectural Institute of Japan (AIJ), and the Asian Control Association (ACA). He was the Recipient of the International Federation of Automatic Control (IFAC) Control Engineering Practice Paper Prize in 1999 (jointly with M. Wu and M. Nakano).

Kou Miyamoto (Member, IEEE) received the B.S. degree in engineering from University of Tsukuba, Japan in 2014, and the M.S. and Ph.D. degrees in engineering from Tokyo Institute of Technology in 2016 and 2019, respectively.

In 2019, he joined the Institute of Technology in Shimizu Corporation, where he is currently a Researcher. His research interests include active control for civil structures, structural control, and robust control for buildings.

Dr. Miyamoto is a Member of Japan Society of Mechanical Engineers (JSME) and Architectural Institute Japan (AIJ).

Qing-Long Han (Fellow, IEEE) received the B.Sc. degree in mathematics from Shandong Normal University in 1983, and the M.Sc. and Ph.D. degrees in control engineering from East China University of Science and Technology, in 1992 and 1997, respectively. He is Pro Vice-Chancellor (Research Quality) and a Distinguished Professor at Swinburne University of Technology, Australia. He held various academic and management positions at Griffith University and Central Queensland University, Australia. His research interests include networked control systems, multi-agent systems, time-delay systems, smart grids, unmanned surface vehicles, and neural networks.

Professor Han was awarded The 2021 Norbert Wiener Award (the Highest Award in systems science and engineering, and cybernetics) and The 2021 M. A. Sargent Medal (the Highest Award of the Electrical College Board of Engineers Australia). He was the recipient of The 2022 IEEE Systems, Man, and Cybernetics Society Andrew P. Sage Best Transactions Paper Award, The 2021 IEEE/CAA Journal of Automatica Sinica Norbert Wiener Review Award, The 2020 IEEE Systems, Man, and Cybernetics Society Andrew P. Sage Best Transactions Paper Award, The 2020 IEEE Transactions on Industrial Informatics Outstanding Paper Award, and The 2019 IEEE Systems, Man, and Cybernetics Society Andrew P. Sage Best Transactions Paper Award.

Professor Han is a Member of the Academia Europaea (The Academy of Europe). He is a Fellow of The International Federation of Automatic Control (IFAC) and a Fellow of The Institution of Engineers Australia (IEAust). He is a Highly Cited Researcher in both Engineering and Computer Science (Clarivate). He has served as an AdCom Member of IEEE Industrial Electronics Society (IES), a Member of IEEE IES Fellows Committee, and Chair of IEEE IES Technical Committee on Networked Control Systems. Currently, he is Editor-in-Chief of *IEEE/CAA Journal of Automatica Sinica*, Co-Editor-in-Chief of *IEEE Transactions on Industrial Informatics*, and Co-Editor of *Australian Journal of Electrical and Electronic Engineering*.

Min Wu (Fellow, IEEE) received the B.S. and M.S. degrees from Central South University in 1983 and 1986, respectively, and the Ph.D. degree from Tokyo Institute of Technology, Japan, in 1999, all in engineering.

He was a Faculty Member of the School of Information Science and Engineering, Central South University, from 1986 to 2014, and became a Professor in 1994. In 2014, he joined the China University of Geosciences, where he is currently a Professor of Control Science and Engineering in the School of Automation. He was a Visiting Scholar with the Department of Electrical Engineering, Tohoku University, Japan, from 1989 to 1990, and a Visiting Research Scholar with the Department of Control and Systems Engineering, Tokyo Institute of Technology, from 1996 to 1999. He was a Visiting Professor with the School of

Mechanical, Materials, Manufacturing Engineering and Management, University of Nottingham, U.K., from 2001 to 2002. His current research interests include robust control, process control, and intelligent systems. Dr. Wu is a Fellow of the Chinese Association of Automation (CAA).

He received the International Federation of Automatic Control (IFAC) Control Engineering Practice Prize Paper Award in 1999 (together with M. Nakano and J. She).

Hiroshi Hashimoto (Member, IEEE) received the Ph.D. degree in science engineering from Waseda University, Japan, in 1990.

He is currently a Professor at the School of Industrial Technology, Advanced Institute of Industrial Technology, Japan, where he researches intelligent robots, cybernetic interfaces, vision systems, welfare technology, and e-learning. His current research interests include mechatronics and the application of control theory.

Dr. Hashimoto is a Member of the Society of Instrument and Control Engineers (SICE) and the Institute of Electrical Engineers of Japan (IEEJ).

Qing-Guo Wang received the Ph.D. degree in 1987 with highest honor from Zhejiang University.

He is a Member of Academy of Science of South Africa. He is currently a Chair Professor with BNU-HKBU United International College; a Professor with BNU-UIC Institute of Artificial Intelligence and Future Networks; and a Professor with Beijing Normal University.

He was AvH Research Fellowship of Germany from 1990 to 1992. From 1992 to 2015, he was with Department of Electrical and Computer Engineering of the National University of Singapore, where he became a Full Professor in 2004. He was a Distinguished Professor with Institute for Intelligent Systems, University of Johannesburg, South Africa, 2015–2020. His research lies in the field of automation/AI with focuses on modeling, estimation, prediction, control, and optimization. He has published 360+ technical papers in international journals and seven research monographs. He received nearly 20000 citations with h-index of 77. He was presented with the award of the most cited article of the journal "Automatica" in 2006–2010 and was in the Thomson Reuters list of the highly cited researchers 2013 in Engineering. He received the prize of the most influential paper of the 30 years of the journal "Control Theory and Applications" in 2014. He was on Stanford University list of World's Top 2% Scientists 2020 (both career and year). He is currently the deputy Editor-in-Chief of the *ISA Transactions* (USA).